

EXPERIMENTS ON IMPROVING THE
EFFICIENCY OF THE BEVATRON ION SOURCE

TROY EDWARD STONE

Library
U. S. Naval Postgraduate School
Monterey, California

1999 1000 1001 1002 1003 1004 1005 1006 1007 1008 1009 1010 1011 1012 1013 1014 1015 1016 1017 1018 1019 1020 1021 1022 1023 1024 1025 1026 1027 1028 1029 1030 1031 1032 1033 1034 1035 1036 1037 1038 1039 1040 1041 1042 1043 1044 1045 1046 1047 1048 1049 1050 1051 1052 1053 1054 1055 1056 1057 1058 1059 1060 1061 1062 1063 1064 1065 1066 1067 1068 1069 1070 1071 1072 1073 1074 1075 1076 1077 1078 1079 1080 1081 1082 1083 1084 1085 1086 1087 1088 1089 1090 1091 1092 1093 1094 1095 1096 1097 1098 1099 1100 1101 1102 1103 1104 1105 1106 1107 1108 1109 1110 1111 1112 1113 1114 1115 1116 1117 1118 1119 1120 1121 1122 1123 1124 1125 1126 1127 1128 1129 1130 1131 1132 1133 1134 1135 1136 1137 1138 1139 1140 1141 1142 1143 1144 1145 1146 1147 1148 1149 1150 1151 1152 1153 1154 1155 1156 1157 1158 1159 1160 1161 1162 1163 1164 1165 1166 1167 1168 1169 1170 1171 1172 1173 1174 1175 1176 1177 1178 1179 1180 1181 1182 1183 1184 1185 1186 1187 1188 1189 1190 1191 1192 1193 1194 1195 1196 1197 1198 1199 1200 1201 1202 1203 1204 1205 1206 1207 1208 1209 1210 1211 1212 1213 1214 1215 1216 1217 1218 1219 1220 1221 1222 1223 1224 1225 1226 1227 1228 1229 1230 1231 1232 1233 1234 1235 1236 1237 1238 1239 1240 1241 1242 1243 1244 1245 1246 1247 1248 1249 1250 1251 1252 1253 1254 1255 1256 1257 1258 1259 1260 1261 1262 1263 1264 1265 1266 1267 1268 1269 1270 1271 1272 1273 1274 1275 1276 1277 1278 1279 1280 1281 1282 1283 1284 1285 1286 1287 1288 1289 1290 1291 1292 1293 1294 1295 1296 1297 1298 1299 1300 1301 1302 1303 1304 1305 1306 1307 1308 1309 1310 1311 1312 1313 1314 1315 1316 1317 1318 1319 1320 1321 1322 1323 1324 1325 1326 1327 1328 1329 1330 1331 1332 1333 1334 1335 1336 1337 1338 1339 1340 1341 1342 1343 1344 1345 1346 1347 1348 1349 1350 1351 1352 1353 1354 1355 1356 1357 1358 1359 1360 1361 1362 1363 1364 1365 1366 1367 1368 1369 1370 1371 1372 1373 1374 1375 1376 1377 1378 1379 1380 1381 1382 1383 1384 1385 1386 1387 1388 1389 1390 1391 1392 1393 1394 1395 1396 1397 1398 1399 1400 1401 1402 1403 1404 1405 1406 1407 1408 1409 1410 1411 1412 1413 1414 1415 1416 1417 1418 1419 1420 1421 1422 1423 1424 1425 1426 1427 1428 1429 1430 1431 1432 1433 1434 1435 1436 1437 1438 1439 1440 1441 1442 1443 1444 1445 1446 1447 1448 1449 1450 1451 1452 1453 1454 1455 1456 1457 1458 1459 1460 1461 1462 1463 1464 1465 1466 1467 1468 1469 1470 1471 1472 1473 1474 1475 1476 1477 1478 1479 1480 1481 1482 1483 1484 1485 1486 1487 1488 1489 1490 1491 1492 1493 1494 1495 1496 1497 1498 1499 1500 1501 1502 1503 1504 1505 1506 1507 1508 1509 1510 1511 1512 1513 1514 1515 1516 1517 1518 1519 1520 1521 1522 1523 1524 1525 1526 1527 1528 1529 1530 1531 1532 1533 1534 1535 1536 1537 1538 1539 1540 1541 1542 1543 1544 1545 1546 1547 1548 1549 1550 1551 1552 1553 1554 1555 1556 1557 1558 1559 1560 1561 1562 1563 1564 1565 1566 1567 1568 1569 1570 1571 1572 1573 1574 1575 1576 1577 1578 1579 1580 1581 1582 1583 1584 1585 1586 1587 1588 1589 1590 1591 1592 1593 1594 1595 1596 1597 1598 1599 1600 1601 1602 1603 1604 1605 1606 1607 1608 1609 1610 1611 1612 1613 1614 1615 1616 1617 1618 1619 1620 1621 1622 1623 1624 1625 1626 1627 1628 1629 1630 1631 1632 1633 1634 1635 1636 1637 1638 1639 1640 1641 1642 1643 1644 1645 1646 1647 1648 1649 1650 1651 1652 1653 1654 1655 1656 1657 1658 1659 1660 1661 1662 1663 1664 1665 1666 1667 1668 1669 1670 1671 1672 1673 1674 1675 1676 1677 1678 1679 1680 1681 1682 1683 1684 1685 1686 1687 1688 1689 1690 1691 1692 1693 1694 1695 1696 1697 1698 1699 1700 1701 1702 1703 1704 1705 1706 1707 1708 1709 1710 1711 1712 1713 1714 1715 1716 1717 1718 1719 1720 1721 1722 1723 1724 1725 1726 1727 1728 1729 1730 1731 1732 1733 1734 1735 1736 1737 1738 1739 1740 1741 1742 1743 1744 1745 1746 1747 1748 1749 1750 1751 1752 1753 1754 1755 1756 1757 1758 1759 1760 1761 1762 1763 1764 1765 1766 1767 1768 1769 1770 1771 1772 1773 1774 1775 1776 1777 1778 1779 1780 1781 1782 1783 1784 1785 1786 1787 1788 1789 1790 1791 1792 1793 1794 1795 1796 1797 1798 1799 1800 1801 1802 1803 1804 1805 1806 1807 1808 1809 1810 1811 1812 1813 1814 1815 1816 1817 1818 1819 1820 1821 1822 1823 1824 1825 1826 1827 1828 1829 1830 1831 1832 1833 1834 1835 1836 1837 1838 1839 1840 1841 1842 1843 1844 1845 1846 1847 1848 1849 1850 1851 1852 1853 1854 1855 1856 1857 1858 1859 1860 1861 1862 1863 1864 1865 1866 1867 1868 1869 1870 1871 1872 1873 1874 1875 1876 1877 1878 1879 1880 1881 1882 1883 1884 1885 1886 1887 1888 1889 1890 1891 1892 1893 1894 1895 1896 1897 1898 1899 1900 1901 1902 1903 1904 1905 1906 1907 1908 1909 1910 1911 1912 1913 1914 1915 1916 1917 1918 1919 1920 1921 1922 1923 1924 1925 1926 1927 1928 1929 1930 1931 1932 1933 1934 1935 1936 1937 1938 1939 1940 1941 1942 1943 1944 1945 1946 1947 1948 1949 1950 1951 1952 1953 1954 1955 1956 1957 1958 1959 1960 1961 1962 1963 1964 1965 1966 1967 1968 1969 1970 1971 1972 1973 1974 1975 1976 1977 1978 1979 1980 1981 1982 1983 1984 1985 1986 1987 1988 1989 1990 1991 1992 1993 1994 1995 1996 1997 1998 1999 2000 2001 2002 2003 2004 2005 2006 2007 2008 2009 2010 2011 2012 2013 2014 2015 2016 2017 2018 2019 2020 2021 2022 2023 2024 2025 2026 2027 2028 2029 2030 2031 2032 2033 2034 2035 2036 2037 2038 2039 2040 2041 2042 2043 2044 2045 2046 2047 2048 2049 2050 2051 2052 2053 2054 2055 2056 2057 2058 2059 2060 2061 2062 2063 2064 2065 2066 2067 2068 2069 2070 2071 2072 2073 2074 2075 2076 2077 2078 2079 2080 2081 2082 2083 2084 2085 2086 2087 2088 2089 2090 2091 2092 2093 2094 2095 2096 2097 2098 2099 2100 2101 2102 2103 2104 2105 2106 2107 2108 2109 2110 2111 2112 2113 2114 2115 2116 2117 2118 2119 2120 2121 2122 2123 2124 2125 2126 2127 2128 2129 2130 2131 2132 2133 2134 2135 2136 2137 2138 2139 2140 2141 2142 2143 2144 2145 2146 2147 2148 2149 2150 2151 2152 2153 2154 2155 2156 2157 2158 2159 2160 2161 2162 2163 2164 2165 2166 2167 2168 2169 2170 2171 2172 2173 2174 2175 2176 2177 2178 2179 2180 2181 2182 2183 2184 2185 2186 2187 2188 2189 2190 2191 2192 2193 2194 2195 2196 2197 2198 2199 2200 2201 2202 2203 2204 2205 2206 2207 2208 2209 2210 2211 2212 2213 2214 2215 2216 2217 2218 2219 2220 2221 2222 2223 2224 2225 2226 2227 2228 2229 2230 2231 2232 2233 2234 2235 2236 2237 2238 2239 2240 2241 2242 2243 2244 2245 2246 2247 2248 2249 2250 2251 2252 2253 2254 2255 2256 2257 2258 2259 2260 2261 2262 2263 2264 2265 2266 2267 2268 2269 2270 2271 2272 2273 2274 2275 2276 2277 2278 2279 2280 2281 2282 2283 2284 2285 2286 2287 2288 2289 2290 2291 2292 2293 2294 2295 2296 2297 2298 2299 2300 2301 2302 2303 2304 2305 2306 2307 2308 2309 2310 2311 2312 2313 2314 2315 2316 2317 2318 2319 2320 2321 2322 2323 2324 2325 2326 2327 2328 2329 2330 2331 2332 2333 2334 2335 2336 2337 2338 2339 2340 2341 2342 2343 2344 2345 2346 2347 2348 2349 2350 2351 2352 2353 2354 2355 2356 2357 2358 2359 2360 2361 2362 2363 2364 2365 2366 2367 2368 2369 2370 2371 2372 2373 2374 2375 2376 2377 2378 2379 2380 2381 2382 2383 2384 2385 2386 2387 2388 2389 2390 2391 2392 2393 2394 2395 2396 2397 2398 2399 2400 2401 2402 2403 2404 2405 2406 2407 2408 2409 2410 2411 2412 2413 2414 2415 2416 2417 2418 2419 2420 2421 2422 2423 2424 2425 2426 2427 2428 2429 2430 2431 2432 2433 2434 2435 2436 2437 2438 2439 2440 2441 2442 2443 2444 2445 2446 2447 2448 2449 2450 2451 2452 2453 2454 2455 2456 2457 2458 2459 2460 2461 2462 2463 2464 2465 2466 2467 2468 2469 2470 2471 2472 2473 2474 2475 2476 2477 2478 2479 2480 2481 2482 2483 2484 2485 2486 2487 2488 2489 2490 2491 2492 2493 2494 2495 2496 2497 2498 2499 2500 2501 2502 2503 2504 2505 2506 2507 2508 2509 2510 2511 2512 2513 2514 2515 2516 2517 2518 2519 2520 2521 2522 2523 2524 2525 2526 2527 2528 2529 2530 2531 2532 2533 2534 2535 2536 2537 2538 2539 2540 2541 2542 2543 2544 2545 2546 2547 2548 2549 2550 2551 2552 2553 2554 2555 2556 2557 2558 2559 2560 2561 2562 2563 2564 2565 2566 2567 2568 2569 2570 2571 2572 2573 2574 2575 2576 2577 2578 2579 2580 2581 2582 2583 2584 2585 2586 2587 2588 2589 2590 2591 2592 2593 2594 2595 2596 2597 2598 2599 2600 2601 2602 2603 2604 2605 2606 2607 2608 2609 2610 2611 2612 2613 2614 2615 2616 2617 2618 2619 2620 2621 2622 2623 2624 2625 2626 2627 2628 2629 2630 2631 2632 2633 2634 2635 2636 2637 2638 2639 2640 2641 2642 2643 2644 2645 2646 2647 2648 2649 2650 2651 2652 2653 2654 2655 2656 2657 2658 2659 2660 2661 2662 2663 2664 2665 2666 2667 2668 2669 2670 2671 2672 2673 2674 2675 2676 2677 2678 2679 2680 2681 2682 2683 2684 2685 2686 2687 2688 2689 2690 2691 2692 2693 2694 2695 2696 2697 2698 2699 2700 2701 2702 2703 2704 2705 2706 2707 2708 2709 2710 2711 2712 2713 2714 2715 2716 2717 2718 2719 2720 2721 2722 2723 2724 2725 2726 2727 2728 2729 2730 2731 2732 2733 2734 2735 2736 2737 2738 2739 2740 2741 2742 2743 2744 2745 2746 2747 2748 2749 2750 2751 2752 2753 2754 2755 2756 2757 2758 2759 2760 2761 2762 2763 2764 2765 2766 2767 2768 2769 2770 2771 2772 2773 2774 2775 2776 2777 2778 2779 2780 2781 2782 2783 2784 2785 2786 2787 2788 2789 2790 2791 2792 2793 2794 2795 2796 2797 2798 2799 2800 2801 2802 2803 2804 2805 2806 2807 2808 2809 2810 2811 2812 2813 2814 2815 2816 2817 2818 2819 2820 2821 2822 2823 2824 2825 2826 2827 2828 2829 2830 2831 2832 2833 2834 2835 2836 2837 2838 2839 2840 2841 2842 2843 2844 2845 2846 2847 2848 2849 2850 2851 2852 2853 2854 2855 2856 2857 2858 2859 2860 2861 2862 2863 2864 2865 2866 2867 2868 2869 2870 2871 2872 2873 2874 2875 2876 2877 2878 2879 2880 2881 2882 2883 2884 2885 2886 2887 2888 2889 2890 2891 2892 2893 2894 2895 2896 2897 2898 2899 2900 2901 2902 2903 2904 2905 2906 2907 2908 2909 2910 2911 2912 2913 2914 2915 2916 2917 2918 2919 2920 2921 2922 2923 2924 2925 2926 2927 2928 2929 2930 2931 2932 2933 2934 2935 2936 2937 2938 2939 2940 2941 2942 2943 2944 2945 2946 2947 2948 2949 2950 2951 2952 2953 2954 2955 2956 2957 2958 2959 2960 2961 2962 2963 2964 2965 2966 2967 2968 2969 2970 2971 2972 2973 2974 2975 2976 2977 2978 2979 2980 2981 2982 2983 2984 2985 2986 2987 2988 2989 2990 2991 2992 2993 2994 2995 2996 2997 2998 2999 3000 3001 3002 3003 3004 3005 3006 3007 3008 3009 3010 3011 3012 3013 3014 3015 3016 3017 3018 3019 3020 3021 3022 3023 3024 3025 3026 3027 3028 3029 3030 3031 3032 3033 3034 3035 3036 3037 3038 3039 3040 3041 3042 3043 3044 3045 3046 3047 3048 3049 3050 3051 3052 3053 3054 3055 3056 3057 3058 3059 3060 3061 3062 3063 3064 3065 3066 3067 3068 3069 3070 3071 3072 3073 3074 3075 3076 3077 3078 3079 3080 3081 3082 3083 3084 3085 3086 3087 3088 3089 3090 3091 3092 3093 3094 3095 3096 3097 3098 3099 3100 3101 3102 3103 3104 3105 3106 3107 3108 3109 3110 3111 3112 3113 3114 3115 3116 3117 3118 3119 3120 3121 3122 3123 3124 3125 3126 3127 3128 3129 3130 3131 3132 3133 3134 3135 3136 3137 3138 3139 3140 3141 3142 3143 3144 3145 3146 3147 3148 3149 3150 3151 3152 3153 3154 3155 3156 3157 3158 3159 3160 3161 3162 3163 3164 3165 3166 3167 3168 3169 3170 3171 3172 3173 3174 3175 3176 3177 3178 3179 3180 3181 3182 3183 3184 3185 3186 3187 3188 3189 3190 3191 3192 3193 3194 3195 3196 3197 3198 3199 3200 3201 3202 3203 3204 3205 3206 3207 3208 3209 3210 3211 3212 3213 3214 3215 3216 3217 3218 3219 3220 3221 3222 3223 3224 3225 3226 3227 3228 3229 3230 3231 3232 3233 3234 3235 3236 3237 3238 3239 3240 3241 3242 3243 3244 3245 3246 3247 3248 3249 3250 3251 3252 3253 3254 3255 3256 3257 3258 3259 3260 3261 3262 3263 3264 3265 3266 3267 3268 3269 3270 3271 3272 3273 3274 3275 3276 3277 3278 3279 3280 3281 3282 3283 3284 3285 3286 3287 3288 3289 3290 3291 3292 3293 3294 3295 3296 3297 3298 3299 3300 3301 3302 3303 3304 3305 3306 3307 3308 3309 3310 3311 3312 3313 3314 3315 3316 3317 3318 3319 3320 3321 3322 3323 3324 3325 3326 3327 3328 3329 3330 3331 3332 3333 3334 3335 3336 3337 3338 3339 3340 3341 3342 3343 3344 3345 3346 3347 3348 3349 3350 3351 3352 3353 3354 3355 3356 3357 3358 3359 3360 3361 3362 3363 3364 3365 3366 3367 3368 3369 3370 3371 3372 3373 3374 3375 3376 3377 3378 3379 3380 3381 3382 3383 3384 3385 3386 3387 3388 3389 3390 3391 3392 3393 3394 3395 3396 3397 3398 3399 3400 3401 3402 3403 3404 3405 3406 3407 3408 3409 3410 3411 3412 3413 3414 3415 3416 3417 3418 3419 3420 3421 3422 3423 3424 3425 3426 3427 3428 3429 3430 3431 3432 3433 3434 3435 3436 3437 3438 3439 3440 3441 3442 3443 3444 3445 3446 3447 3448 3449 3450 3451 3452 3453 3454 3455

EXPERIMENTS ON IMPROVING THE EFFICIENCY
OF THE BEVATRON ION SOURCE

by

Troy Edward Stone

Lieutenant, United States Navy

Submitted in partial fulfillment
of the requirements
for the degree of
MASTER OF SCIENCE
IN
PHYSICS

United States Naval Postgraduate School
Monterey, California

1 9 5 5

77-1

5765

EXPERIMENTAL OR IMPROVED THE EXISTING
OF THE REVENUE FOR SPACE

70

For the purpose of the

Department, the following

Department of the Interior
in the Department
for the purpose of
the Department of
the Department of
the Department of
the Department of

Department of the Interior
for the purpose of the

1918

This work is accepted as fulfilling

the thesis requirements for the degree of

MASTER OF SCIENCE

IN

PHYSICS

from the

United States Naval Postgraduate School

This work is intended as a guide
to the study of the subject.

MASTERS OF ARTS

IN

1900

1900

United States of America

ABSTRACT

Library
U. S. Naval Postgraduate School
Monterey, California

A study has been conducted to determine the focal properties of an ion source that is typical of those used with the Bevatron. Beam-intensity patterns have been obtained for various focusing conditions. The effects of space-charge repulsion and lens aberration have been investigated. Losses through Coulomb scattering on residual gas molecules have been observed, and a curve showing variation of these losses with variation of energy through the focus electrode has been obtained. Pressure throughout the accelerating column was found to be an important factor, and losses occasioned through slight increases in the normal operating pressure have been recorded.

All previous ion sources for the Bevatron have been designed for presentation of a real image to the subsequent injection system. A virtual-image source has been designed, constructed and tested on the Bevatron.

PREFACE

A continuing and intensive effort is being made to increase the magnitude of the output beam of the Bevatron. Refinements in the machine itself during the past year have resulted in a current intensity approaching 10^{10} protons per pulse, a most significant improvement; but considerably better performance than this is envisioned. Increasing the output and (or) improving the efficiency of the Bevatron^{*} ion source is one way of attaining more beam, and to this end work has been conducted during the past year by the writer.

This experimentation was conducted under the guidance of Dr. B. B. Kinsey, formerly of the Chalk River Atomic Energy Project and during the past year a visiting scientist at the University of California Radiation Laboratory. Frequent recourse has been made to the knowledge and experience of Bruce Cork of the Bevatron staff. The writer is particularly indebted to them for their enlightenment, assistance, and encouragement during the course of this work.

The writer wishes to thank Professor N. L. Oleson of the U. S. Naval Postgraduate School for his assistance in the preparation of this paper.

This work was conducted under the auspices of the U. S. Atomic Energy Commission while the writer was attached to the University of California Radiation Laboratory.

TABLE OF CONTENTS

Item	Title	Page
Abstract	ii
Preface	iii
List of Illustrations	v
Chapter I	Introduction	1
Chapter II	Focal Properties of a Typical Ion Source	5
Chapter III	Losses through Space-Charge Repulsion, Lens Aberration, Coulomb Scattering, and Residual Gas	10
Chapter IV	Design and Test of a Virtual-Image Ion Source	16
Bibliography	20

LIST OF ILLUSTRATIONS

Figure		Page
1.	Block Diagram of Ion Source	21
2.	Cross Section of Arc Chamber	22
3.	Focusing Action of Three Electrodes	23
4.	Block Diagram of Bevatron Injection System	24
5.	Original Faraday Cup, Shield with 3/8-inch Hole	25
6.	Faraday Cup, Long Shield	25
7.	Faraday Cup, Special Shield	25
8.	Mechanical Advantage of Cup Movement	26
9.	Beam-Intensity Cross Sections, Variable-Focus Electrode Voltage	27
10.	Spreading of Originally Parallel Proton Beam Due to Space Charge	28
11.	Ion Trap	29
12.	Beam-Intensity Cross Sections, Space- Charge Effects	30
13.	Spherical Aberration	31
14.	Chromatic Aberration	31
15.	Beam-Intensity Cross Sections, Aberration Effects	32
16.	Total Current vs. Energy, Coulomb Losses	33

LIST OF ILLUSTRATIONS

Page	Figure
11	Block Diagram of the System
12	Block Diagram of the System
13	Block Diagram of the System
14	Block Diagram of the System
15	Block Diagram of the System
16	Block Diagram of the System
17	Block Diagram of the System
18	Block Diagram of the System
19	Block Diagram of the System
20	Block Diagram of the System
21	Block Diagram of the System
22	Block Diagram of the System
23	Block Diagram of the System
24	Block Diagram of the System
25	Block Diagram of the System
26	Block Diagram of the System
27	Block Diagram of the System
28	Block Diagram of the System
29	Block Diagram of the System
30	Block Diagram of the System
31	Block Diagram of the System
32	Block Diagram of the System
33	Block Diagram of the System
34	Block Diagram of the System
35	Block Diagram of the System
36	Block Diagram of the System
37	Block Diagram of the System

CHAPTER I

INTRODUCTION

An ion source provides the flow of ions which are the bombarding particles of an accelerator. The kinds of ions that are utilized by present accelerators are protons (${}_1\text{H}^1$), deuterons (${}_1\text{H}^2$), and alpha particles (${}_2\text{He}^4$). Lithium ions have been used infrequently. In some cases, ions of tritium (${}_1\text{H}^3$) or light helium (${}_2\text{He}^3$) are desired, but these are generally obtained by nuclear processes rather than from an ion source. Since the Bevatron is designed for the acceleration of protons, this paper will be confined to ion sources that deliver protons.

The original ion source used in the Bevatron was basically the same as that developed by Gow and Foster [1] for the Radiation Laboratory, University of California 32-Mev proton linear accelerator. With only minor modifications this design, shown in Fig. 1, is still in use. The arc chamber used in this source, shown in detail in Fig. 2, is of the type generally known as a Penning or Phillips ion gauge [2]. Such an arc chamber was chosen because it has one of the most simple geometrical forms that will produce a stable discharge. Aside from simplicity, its advantages are low-pressure operation, high efficiency, no filament, and small physical size. Axial extraction of the ions is employed because it is the simplest means of withdrawal. The three focusing electrodes are placed in typical electron-gun fashion, and are referred to throughout this paper as the probe, the focus, and the accelerating electrodes.

Atomic hydrogen gas that is to be ionized in the arc chamber of the source is obtained by passing hydrogen gas through a palladium leak. This atomic gas is immediately introduced into the arc chamber, where a strong electric field is utilized to strike an arc between anode and cathode. An electron released from a cathode, which is made of uncoated aluminum, is accelerated toward the anode. As the entire arc chamber is centered in a coil which provides an axial magnetic field of high intensity, radial motion of the electron is constrained by this

field. The constraint may be such that the electron is accelerated into the anode, coasts through the field-free region within, loses energy through collisions with the gas, and emerges from the other end with somewhat less energy than it gained in its initial acceleration. It is reflected by the electric field, is constrained again by the magnetic field, re-enters the anode, and continues its axial oscillation. During its oscillation it produces several ion pairs, losing energy of the order of 35 volts per pair, and finally it falls below ionization energy and subsequently is taken up by the anode. Since the initial energy of the electron is several hundred volts, it produces approximately ten ions within the anode during its oscillations. These ions are also constrained by the magnetic field so that their principal motion is axial. Eventually, they come to one end of the anode, where they are accelerated into the corresponding cathode. Some of those accelerated into the forward cathode pass through the exit hole and become useful proton beam.

A proton of several hundred volts energy incident on the cathode surface has a finite probability of releasing a secondary electron. Electrons so released will have life cycles as described above. No good data are available on the magnitude of the proton-to-secondary-electron ratio for aluminum oxide, but Gow and Foster [1] estimate that it lies between five and ten. If more ions than this figure are produced by the first electron, the discharge will increase in intensity until limited by other mechanisms.

A fundamental problem within the arc chamber is that of the mean free path for ionization. Let us call it λ_i , and d the mean length of an electron path from cathode to anode. For a single electron emitted by the cathode the probability of ionization is approximately d/λ_i , where d is considerably less than λ_i . If the pressure in the arc chamber were equal to that in the accelerator, λ_i would be equal to several hundred meters. If this were the case, the rate of ionization would be exceedingly low. If we take d equal to ten centimeters and λ_i as 200 meters, we will get approximately one ion for every 2000 electrons. And since the exit hole in the cathode through which ions are drawn is only 0.050 inch in diameter, the rate of removal of ions is generally low. Considering probabilities of production and of extraction, we will

get relatively few useful ions.

To state it simply, the pressure in the injection system and through the Bevatron must be sufficiently low to allow the accelerating ions to travel from the source to the target without colliding with residual neutral atoms. On the other hand, electrons emitted by the cathode must have a high probability of colliding with atomic hydrogen atoms within the arc chamber in order to give a high rate of ionization. These requirements are met by (a) utilizing a high-speed pumping system which permits relatively high pressure within the arc chamber, and (b) forcing the electrons to follow complicated paths before reaching the anode, as described above.

Pulses of current through the arc chamber are provided by a three-kilovolt power supply that is capable of three amperes of current during millisecond pulses, such pulses coming twice per second. Thus pulses of protons, mixed with ionized molecular hydrogen, are emitted from the exit hole in the cathode with the same frequency.

The presence of ionized molecular hydrogen is, of course, undesirable. Such ions are not acceptable for the Bevatron, which is synchronized for the charge and mass of the proton, and they take the place of protons in the ion stream. Several investigators [3] have sought to increase the output of similar sources by introducing impurities that ionize at low voltage, such as mercury vapor. They found that these impurities generally give a manifold increase of the beam current, but magnetic analysis shows that almost all the ions arise from the impurities. Useful current is actually decreased.

The proton-to-molecular-hydrogen ratio can be varied within limits, however. In general, higher arc currents, stronger magnetic fields, and lower arc-chamber pressures give the more favorable ratios. Under good operating conditions with the type of chambers utilized in these experiments, 75 percent protons are obtained, but under normal operating conditions a common figure is 60 percent protons.

The size of the exit hole in the arc chamber is necessarily a compromise. Although the number of protons emitted increases with increase in aperture size, the increase realized is somewhat less than

directly proportional to the area of the aperture [4] . And a larger hole results in higher pressure throughout the subsequent system, which is obviously undesirable, and offers a larger object to the focusing system, which results in a larger image spot. Larger holes also complicate control of the plasma emission surface, such control being accomplished through adjustment of the probe electrode voltage. With no probe voltage, the plasma surface protrudes from the exit hole in tongue fashion. Increasing the probe voltage causes the plasma surface to retreat back into the hole until, under the most favorable emission conditions, the surface is perpendicular to the axis of the source. If the hole is made too large, however, the plasma can no longer be forced back properly by probe voltage, the plasma surface is not perpendicular, and beam current decreases. The exit-hole diameter that has been found to be the best compromise is 0.050 inch.

The focusing action of the three electrodes is shown in Fig. 3. Protons emerging from the exit hole are accelerated to approximately 20 kilovolts by the probe electrode, decelerated to about eight kilovolts in the focus electrode, and accelerated to 45 or 50 kilovolts in the accelerating electrode. With these voltage settings, a real image is obtained approximately one foot beyond the accelerating electrode.

The output beam from the ion source goes into a Cockcroft-Walton column, (refer to Fig. 4), which accelerates the protons to 500 kilovolts. A turning magnet then deflects the beam 20° and sends it into the buncher, a resonator which increases the height of the proton pulse and decreases its width. The beam then enters the linear accelerator to be raised to ten Mev and, finally, is turned 35° by an electrostatic inflector and injected into the Bevatron proper.

Each of the stages subsequent to the ion source constitutes a focusing system, and the combination of these systems is a compound lens of great complexity. It is thus to be expected that the maximum current reading immediately beyond the ion source or at the end of the Cockcroft-Walton column will not necessarily result in the highest current output for the Bevatron. Indeed, the requirements of the Bevatron are unique, and the efficacy of a source can only be determined by trial and error settings while it is pulsing into the Bevatron.

CHAPTER II

FOCAL PROPERTIES OF A TYPICAL ION SOURCE

The purpose of the experimentation herein described was not to improve the design of the arc chamber, whose operation is described in some detail in the previous chapter, but rather to study means of controlling the beam obtained from such a chamber. The source selected for this study is identical to the one employed in the Bevatron with the exception of the diameter of the focusing electrodes, which are two inches in the former and 1-1/4 inches in the latter. Variation in total output with variation of the focusing-electrode voltages was of interest and was investigated, but the main effort was directed toward obtaining beam-intensity patterns that would show the focal properties of the three-electrode system.

1. Operating conditions.

The pressure in the arc chamber during these experiments was 125 ± 25 microns, and the pressure at the end of the accelerating electrode was about 3×10^{-5} millimeters of mercury. Current in the magnet coils surrounding the arc chamber varied from 0.5 to 1.2 amperes, depending upon the setting needed for stable operation, and this resulted in a magnetic field strength within the chamber varying from 500 to 1000 gauss. Voltage across the arc during a pulse was of the order of 300 volts, with the setting of the arc pulser varying from one to two kilovolts as required for stable operation. Arc current varied from one to three amperes, depending upon the requirements of the experiment.

High-current arcs over long periods necessitate frequent replenishment of the oxide layer on the aluminum cathodes. This is done by running the arc on oxygen for a half hour or so. And, from time to time, the aluminum cathodes are found to form compounds, believed to be carbides of aluminum, on their emission surfaces and must be removed and polished. Complications of this sort make settings for a stable arc somewhat variable, but in most cases results obtained were reproducible within ten percent.

2. Measurement techniques.

The first device used for current measurements was a shielded Faraday cup with a $3/8$ -inch entrance hole (see Fig. 5). It was found that making the cup six volts positive with respect to its shield would decrease current readings by as much as 15 percent. Additional positive bias would decrease current readings still farther, at a decreasing rate, with 90 volts bias resulting in current readings 30 percent below the no-bias figure. Such a fluctuation of current readings showed clearly that electron currents were playing a major role in the readings. Before meaningful beam current readings can be obtained, the magnitude of the electron currents must be known and their effect minimized.

The purpose of positive bias is to draw back secondary electrons formed on the cup and prevent their passing out the entrance hole, being accelerated back through the source, and causing erroneous beam-current readings on the high side. A bias of the order of six volts positive should be sufficient to reclaim all secondaries to the cup, and the decrease in observed current for such a bias is almost assuredly due to this action. The further decrease in current with larger biases indicates that secondaries formed on the lip of the entrance hole were being drawn to the cup and causing erroneous readings on the low side.

In order to provide a long field-free region and minimize the effect of secondary electrons formed at the entrance hole, a device shown in Fig. 6 was constructed. Tests on this device showed that multitudinous secondary electrons were formed on the inside surfaces of the shielding cup when the cup was inclined to the beam. So many of these electrons came into the Faraday cup to be recorded that negative current readings were obtained for all but an axial position of the cup. Clearly this was a much poorer design than before.

To minimize both positive and negative errors in current readings, a device shown in Fig. 7 was developed and has been used for the bulk of the data collected. The field-free region between the two entrance holes makes it unlikely that secondaries formed on the lip of the outer hole will find their way to the cup. A positive bias of six volts on the cup makes it unlikely that secondaries formed on the cup will escape and go back through the source. Readings were found to vary less than

15 percent for the range of biases up to 90 volts.

Small permanent magnets placed around the entrance hole of this device might further reduce errors. Thonemann [5] reports success using a magnetic field of several hundred gauss parallel to the surface of his target cup. In this strong field the secondary electrons, which are relatively slow, are immediately sent back to the cup.

3. Beam-intensity patterns.

The measuring device described above was mounted on the end of a rod (see Fig. 8), which passes through a vacuum seal and provides a means of positioning the cup within the vacuum chamber. The rod can be pushed into the vacuum chamber until the cup lies only two inches from the exit of the accelerating electrode, or pulled out until the cup lies next to the vacuum-chamber wall and is 15 inches from the accelerating electrode. When in the latter position, the exposed end of the rod moves 5.6 inches for each inch of movement of the entrance hole on the cup shield. Thus by plotting positions of the free end of the rod, one obtains quite accurate knowledge of the position of the entrance hole within the chamber. To take advantage of this magnification, all readings for beam intensity patterns were made with the cup at its fully withdrawn position. Total beam currents were obtained by integration of the individual currents throughout the observation plane.

The patterns that are shown as Fig. 9 were obtained by leaving all settings constant while varying the voltage on the focus electrode. There is seen to be a sharp focus at five kilovolts with the pattern flattening and spreading out for voltages above and below this setting. The minimum size of the pattern is of the order of one-half inch in diameter, and for this pattern the central peak carries a current of 0.12 milli-ampere through an aperture 0.042 inch in diameter.

A peculiar property of these patterns is the definite ring effect that is noticeable for focus-electrode settings of 6.2 and 7.1 kilovolts. Similar rings are observed with a thick lens in conventional optics, but there they are most prominent when the observing plane lies outside the focal plane of the lens. The patterns herein obtained show pronounced rings only when the observing plane lies inside the focal plane

of the lens system. Similar rings were noted at other times when data of this type were recorded. They are even more noteworthy for the virtual-image source, which is described in Chapter IV.

4. Probe electrode length.

It was believed the distance from the probe hole to the focus electrode might be greater than necessary and that a shorter drift distance within the probe might result in a sharper focus. To carry out this experiment, it was first necessary to determine whether displacement of the magnet to the rear would adversely affect the operation of the arc chamber. It was found that moving the magnet back one and one-eighth inches decreased the beam current by 25 percent. Runs were also made to see what effect displacement of the magnet has on proton content of the beam. This was done with a magnetic deflecting device which permits separate readings of proton and molecular hydrogen currents. It was found that magnet displacement did not significantly affect the ratio of protons to molecular hydrogen.

A probe $5/8$ inch shorter than the usual one was constructed and installed. The arc chamber was moved toward the probe a corresponding distance. The magnet, which lies flush against the back of the source, could not be moved forward, but the effect of this variation of field strength through the arc chamber had been discounted as noted above. Intensity patterns for this arrangement disclosed a decidedly poorer focusing ability for the system, with flat patterns the rule and focus-electrode voltage of little use in sharpening them up.

Lower arc currents were used for additional patterns with the shorter probe. The fact that the focusing ability of the system notably improved with less beam current indicates that the spreading out of the beam in "pancake" fashion is mainly due to space-charge effects.

A shorter probe was decidedly detrimental; it was decided to explore the operation of a longer one. A probe one inch longer than the customary length was installed. Intensity patterns taken with conditions duplicating previous tests with the customary probe indicate that beam current decreases slightly and focusing ability of the system improves somewhat. Neither effect is pronounced enough to establish whether

the longer probe is preferable; the likelihood is that either will serve equally well.

5. Probe-electrode aperture size.

The size of the probe hole that lies over the arc-chamber exit hole has customarily been about 0.1270 inch in diameter. It seemed desirable to determine the gross effects of enlarging and decreasing the size of this hole by 50 percent. A probe with a hole of 0.1890 inch diameter was tested first, and under optimum conditions beam current was down by a factor of eight from that realized with the normal hole. Tests with a probe having a 0.0760-inch hole were equally unrewarding, the total beam current in this case being down by a factor of three. These decreases in beam current are great enough to establish the optimum size probe hole as in the neighborhood of 0.1270 inch.

6. Probe-tip and exit-plate shapes.

The probe has customarily been machined to form a 90° cone with its entrance hole at the apex. The exit plate is customarily a 90° hollow cone. The probe fits concentrically into the exit plate with the tip of the probe spaced about $1/16$ inch from the exit hole. Gow and Foster [1] report that less acute cone angles cause an appreciable fraction of the beam to strike the probe.

Tests were made with the exit plate essentially flat and with the conventional 90° probe. No noteworthy alteration in beam-current output or in focal properties of the system was observed. A probe with a hemispherical surface on its end was developed and used with a hemispherically shaped exit plate of slightly larger radius. This design seemed to be as good in all respects as the others, and in addition it gave less trouble through sparking between the probe and exit plate.

CHAPTER III

LOSSES THROUGH SPACE-CHARGE REPULSION, LENS ABERRATION, COULOMB SCATTERING, AND RESIDUAL GAS

The desired product of this focusing system is an image free of distortions. It is further desirable that a minimum attenuation of the beam occur while it is being focused. A perfect image may be obtained only if the extent of the object and image as well as the inclination of the image-forming proton rays are exceedingly small, if the velocity of the protons is uniform, and if the proton concentration at all points of the path is so small that the mutual repulsion of the protons has negligible effect. If these three conditions are not fulfilled geometrical aberrations, chromatic aberrations, and space-charge defects arise, the result of each being to decrease useful beam current. A further obvious source of image imperfections is mechanical misalignment or defective construction of the electrodes and (or) the exit aperture.

1. Space-charge repulsion.

The ability of a focusing system to obtain a sharp focus is dependent in large measure upon the effect of space-charge repulsion on the beam. Space-charge effects as observed for charged particles have no parallel in light rays. A strong concentration of protons at any point has the effect of reducing the potential or decreasing the speed of the individual protons. In a beam of given cross section, this concentration is inversely proportional to the velocity. Thus space charge plays a role primarily in low-velocity, high-current beams. Here it produces a spreading of the beam, resembling the effect of a negative lens (see Fig. 10).

Let us consider two identical charged particles traveling together at the same speed. They exert on each other two different forces;

(1) an electrostatic repulsion

$$F_R = \left(\frac{1}{4\pi\epsilon_0} \right) \left(\frac{q}{r} \right)^2,$$

and (2) a magnetic attraction, because they correspond to parallel currents

$$F_A = \left(\frac{\mu_o}{4r} \right) \left(\frac{qv}{r} \right)^2 .$$

It may be seen that

$$\frac{F_A}{F_R} = v^2 \mu_o \epsilon_o = \left(\frac{v}{c} \right)^2 .$$

In the case of protons of energy 20 kilovolts, v is only 2×10^6 meters per second, so that F_A/F_R is about 3×10^{-5} , and we see that F_A can be neglected. This would not be the case for electrons of the same energy.

For either electrons or protons the effect of mutual repulsion is far from negligible. For a one-milliamper beam of electrons with an energy of 20 kilovolts, the speed is 8.5×10^7 meters per second and the charge density is 1.2×10^{-11} Coulomb per meter. On the other hand, protons with the same energy have a much lower speed, and their charge density would be 4.5×10^{-10} Coulomb per meter. Thus we see that the space-charge repulsion of a proton beam is much higher than for an electron beam of the same energy, because the charge density is higher and the attractive force is negligible.

A complete treatment of this problem has been made by Fowler and Gibson in "The Production of Intense Beams of Positive Ions." [6] . Their results may be summarized as follows: Consider an initially parallel beam a centimeters in radius; its radius due to space-charge repulsion becomes $2a$, $3a$, $4a$ at distances given by $0.00188A$, $0.00280A$, $0.00358A$, where

$$A = \frac{a U^{3/4} Z^{1/4}}{M^{1/4} I^{1/2}} ,$$

with U expressed in volts and I in amperes; Z is the number of elementary positive charges and M the molecular mass of the ions. Fowler and Gibson state that, for instance, for a proton beam of

20 kilovolts initially 0.375 centimeter in radius, the corresponding distances are 16.8, 24.9, and 31.9 centimeters.

While the above rigorous discussion may well be accurate, Field, Spangenberg, and Helm [7] have shown that positive-ion neutralization of space charge can be attained even at low pressures by means of an "ion trap." This trap (see Fig. 11) consists of suppressor rings at the ends of electrode tubes with a sufficient positive bias to contain positive ions within the electrode. Under these conditions, the investigators report, positive ions are unable to leave the tube, and accumulate in such number that the electron space charge, which would ordinarily depress the potential in the center of the tube, is almost exactly neutralized. Their results show, for instance, that an electron current of 130 milliamperes, traveling 36 centimeters with an energy of 5.7 kilovolts at a pressure of $1/2$ micron, suffered no spread in its diameter. Without the ion trap the beam spread to twice its original diameter.

This ion trap is equally applicable to proton currents, obviously, and the principle further raises the question whether the limiting currents, as described by Fowler and Gibson [6], have any meaning, for negative ions within the tubes were not taken into account. Perhaps there are adequate numbers of negative ions within the focusing electrodes of the ion source to neutralize space-charge effects of the beam and lead to very high limiting currents.

To study space-charge repulsion effects in the test source, intensity patterns were obtained for varying beam currents with all electrode voltages constant. Experimental results show that smaller currents definitely result in a sharper pattern (see Fig. 12). Increasing beam current from 6.1 to 8.7 milliamperes, for instance, cut down the peak current at the center of the pattern by a factor of almost two while the diameter of the pattern increased by a factor of one-half. It is thus apparent that, even though the spreading appears to be less than would be predicted by the rigorous treatment, there is considerable loss through space-charge effects in this source. No attempt was made to employ the "ion trap" to lessen these effects.

2. Lens aberration.

The primary contributions to lens aberration for an electrostatic system are from spherical aberration and chromatic aberration. The former, sometimes called aperture defect, is the only geometric aberration which causes unsharpness of the image on the optic axis (refer to Fig. 13). This aberration results in a circle of confusion about every image point, which is proportional in diameter to the cube of the aperture α of the imaging pencil. In magnitude the spherical aberration is the same over the entire image. It is caused by the fact that rays passing through the outer parts of the lens are refracted somewhat more strongly in proportion to the separation from the axis, returning to the axis at a smaller distance from the lens than rays having a smaller inclination to the axis.

Chromatic aberration results from the fact that the deflecting field of a lens acts for a shorter period of time on a proton of greater velocity. Fast protons are thus less affected and focus at a greater distance from the lens than do slow protons. A spread of the image along the axis is produced by this action, as shown by Fig. 14.

The effect of spherical aberration was investigated by obtaining intensity patterns with identical operating conditions and total beam currents for varying beam-input cross section. In the first case (see Fig. 15), the source operated in the usual fashion. In the second case, a 3/32-inch-diameter collimating hole was placed in the probe 3/4 inch from its tip, and this collimator served to reduce the cross section of the beam as it entered the focusing system. Peak current intensity at the center of the pattern was increased by a factor of four by using the collimator. The diameter of the pattern was half as great with the collimator in as with it out. A large portion of the available beam is screened out by such a collimator, however, and the maximum beam current available with it in use is down by a factor of three.

These experimental results indicate that spherical aberration contributes considerably to the spreading of the beam. Since aberration effects are more pronounced at the edges of a lens field, it might be expected that increasing the diameter of the electrodes would improve

the performance of the source by reducing the spreading of the beam. But increasing the diameter of lenses also reduces their focusing strength, and thus the electrode diameter must be a compromise between these two factors.

Chromatic aberration is doubtless present in the over-all problem, but no means was found for independently investigating its effect. Such aberration is very likely present in the above space-charge and spherical-aberration experiments, but we assume that it does not play a prominent role in the effects attributed to them.

3. Coulomb scattering.

The residual gas molecules within the ion source constitute a target material, albeit quite thin, which the protons must pass through. If a proton in the beam should suffer Coulomb scattering off one of these residual molecules, its loss of energy and change of direction would almost assuredly be great enough for it to be eliminated from the useful beam. Thus it is not a question of whether this effect causes losses, as it may be in the case of space-charge effects, but rather of how large such losses are.

Throughout the runs where beam-intensity patterns were recorded with focus-electrode voltage the only variable, it was noted that less total beam current was observed as the focus voltage decreased. The effect was not obvious, however, until the virtual-image ion source was tested. This source operates in an acceleration-acceleration-deceleration manner, the final or accelerating electrode (using previous terminology) being used as the variable or "focusing" electrode. A plot of total beam current versus accelerating-electrode voltage for the virtual-image source showed a much more noteworthy decrease of current with decreasing voltage.

Coulomb scattering of charged particles by target materials is known to vary in such a way that a plot of $1/E^2$ versus log total bombarding current is a straight line, where E is the energy of the bombarding particles. To correlate the loss in beam current as voltage was decreased with losses due to Coulomb scattering, a plot was made with the arguments $1/E^2$ and log total beam current, where E is the energy

of the accelerating electrode. This plot is shown as Fig. 16, and its close approximation to a straight line confirms that the major contributor to the observed losses is Coulomb scattering.

The ratio between total beam current for accelerating-electrode voltages of ten kilovolts and of five kilovolts is a factor of ten. This clearly demonstrates that the losses incurred through long drift distances at low energy are significant.

In the conventional source the losses from Coulomb scattering are not so pronounced as those discussed above because the drift distance at low energy, i. e. the length of the focus electrode, is not great. Improvement in performance of this source is probable, however, if pressure in the focus electrode can be reduced, or voltage increased, or both.

4. Pressure losses.

The losses through increased pressure in the focusing system are similar in magnitude to and inseparable from Coulomb scattering losses. But it was of interest to observe the gross effects of pressure increase in the system, and data were taken for the conventional and for the virtual-image sources.

An increase of pressure from three to six $\times 10^{-5}$ mm in the focusing system caused a decrease of beam current of 20 percent for the conventional source operating at its usual settings. A similar increase in pressure with the virtual-image source in operation resulted in the loss of 70 percent of the beam. These results confirm a fact well known, that low pressure is of prime importance.

CHAPTER IV

DESIGN AND TEST OF A VIRTUAL-IMAGE ION SOURCE

Experiments conducted during the autumn of 1954 showed that shortening the length of the Cockcroft-Walton column so as to provide a drift distance between the source and column of about two feet resulted in a significant increase in beam current throughout the system. With this new arrangement the exit hole of the arc chamber, which is the position of the object in the composite lens system, was situated more than three feet from the entrance to the Cockcroft-Walton column. This suggested the possibility of employing a virtual-image ion source, which would eliminate the drift distance introduced between source and column and optically provide a virtual image of the exit hole at the same position, relative to the column, as the actual exit hole had been with the conventional source. Such a source would permit the physical position of the exit hole to be at a minimum distance, about 18 inches, from the Cockcroft-Walton entrance. And if it were possible to duplicate the optical characteristics of the conventional source as seen by the Cockcroft-Walton, considerable gain might be realized as the result of eliminating two feet of drift distance, for drift distance is, of itself, necessarily injurious. These reasons, and the fact that a virtual-image source had never been tried on the Bevatron, prompted the attempt to achieve significant improvement in the useful output of the ion source through use of a virtual-image focusing system.

1. Design.

The arc chamber that had been used for the previous experiments was incorporated into the virtual-image source (see Fig. 1), and the physical dimensions of the housing of the focusing electrodes were retained. Thus the new source could be used interchangeably with the old. The changes made to achieve virtual-image performance were in the length and diameter of the electrodes. A three-inch diameter for the tubes was adopted with the hope that gains from lower pressure and less spherical aberration would be greater than any losses occasioned through

weakening of the lenses. One inch was added to the length of the focus electrode, and the accelerating electrode was retained at its usual length by permitting it to protrude an inch farther from the end of the source than before. The probe length was maintained, but the shape of the probe tip and exit plate were hemispherical instead of 90° cones.

To achieve a virtual image, the electrodes are energized to provide an acceleration-acceleration-deceleration action on the protons. Through approximation calculations on the focusing system, it was predicted that, with 20 kilovolts on the probe electrode and 40 kilovolts on the focus electrode, parallel rays would be obtained for an accelerating electrode voltage of about 12 kilovolts. At some higher voltage, something less than 25 kilovolts, the calculations indicated that a virtual image would be achieved about two feet behind the exit hole. With the power supplies that were to be employed, however, adequate latitude of settings was available to insure optimum placement of the virtual image.

2. Test-stand data.

A series of runs was made with probe voltage set at 14 kilovolts and focus voltage at 40 kilovolts. Although a crossover focus was expected with about eight kilovolts on the accelerating electrode, total beam current was so diminished by Coulomb scattering in this low-energy region that the setting for best crossover was effectively masked and total beam currents were deceptively low. If measurements could have been made within the accelerating electrode rather than at a distance two feet beyond, more indicative patterns and higher currents would undoubtedly have been achieved.

Settings of ten kilovolts and slightly above on the accelerating electrode gave much higher total currents, as would be expected with less scattering, and the patterns were spreading out and flattening in a manner indicative of parallel rays, which would be expected with these settings.

No ready means was available on the test stand for determining positions of a virtual image, and further information on the source could only be achieved by operating it with the Bevatron.

3. Bevatron runs.

Before new power supplies for use with the virtual-image source were

measured at the source. The loss was added to the initial value
initially, and the resulting value was added to the total
length of the string. The total length was then added to the
source (the source). The total length was then added to the
the source (the source) and the total length was added to the
The source (the source) and the total length was added to the

an additional source (the source) and the total length was added to the
approximation calculation on the source (the source) and the total length was added to the
with 10 digits on the source (the source) and the total length was added to the
elementary (the source) and the total length was added to the
value of about 11 digits. The total length was added to the
the source (the source) and the total length was added to the
be added to the source (the source) and the total length was added to the
that were to be added to the source (the source) and the total length was added to the
available to the source (the source) and the total length was added to the

1. The source (the source) and the total length was added to the
A source of some size was added to the source (the source) and the total length was added to the
total length of 11 digits. The source (the source) and the total length was added to the
with about 11 digits on the source (the source) and the total length was added to the
was added to the source (the source) and the total length was added to the
the source (the source) and the total length was added to the
the source (the source) and the total length was added to the
with the source (the source) and the total length was added to the
total length of 11 digits on the source (the source) and the total length was added to the
the source (the source) and the total length was added to the

2. The source (the source) and the total length was added to the
Source of the source (the source) and the total length was added to the
the source (the source) and the total length was added to the
the source (the source) and the total length was added to the
the source (the source) and the total length was added to the
the source (the source) and the total length was added to the
the source (the source) and the total length was added to the
the source (the source) and the total length was added to the
the source (the source) and the total length was added to the

3. The source (the source) and the total length was added to the
Source of the source (the source) and the total length was added to the
the source (the source) and the total length was added to the
the source (the source) and the total length was added to the
the source (the source) and the total length was added to the
the source (the source) and the total length was added to the
the source (the source) and the total length was added to the
the source (the source) and the total length was added to the

available, a breakdown of the source in the Bevatron necessitated the installation of the virtual source. It was operated at this time with acceleration-deceleration-acceleration settings, and the best results were obtained when voltages were such as to give a real image. The best performance available with this arrangement showed the current at the end of the Cockcroft-Walton to be comparable with that obtained with the usual source, but total beam out of the linear accelerator was down by a factor of two or three. Therefore, the usual source was replaced in the Bevatron when it was again operative.

Later tests with the virtual-image source operating in its designed fashion--probe voltage 18.5 kilovolts and focus voltage 48 kilovolts--showed a definite maximum current through the Cockcroft-Walton with accelerating voltage at eight kilovolts, a minimum point at 13 kilovolts, and a higher maximum with accelerating voltage at 19 kilovolts. Since from test information a crossover was expected at about 8 kilovolts, this indicates that the first maximum was the crossover or real-image condition, the minimum a case where the rays were essentially parallel, and the larger maximum the desired virtual-image operation. Maximum current through the Cockcroft-Walton with the accelerating voltage in the neighborhood of 19 kilovolts was nine milliamperes, which is somewhat less than the 12 milliamperes obtained under good conditions with the usual source at this position. The maximum available current at the input to the linear accelerator was 2.2 milliamperes, which compares even less favorably with the 6.0 milliamperes that can be obtained with the usual source. Current measurements at the exit of the linear accelerator were ridiculously low, however. Whereas the conventional source may register 300 microamperes at this point, the virtual image source could produce only eight or ten microamperes, a factor of 30 down. The new source was clearly not an improvement.

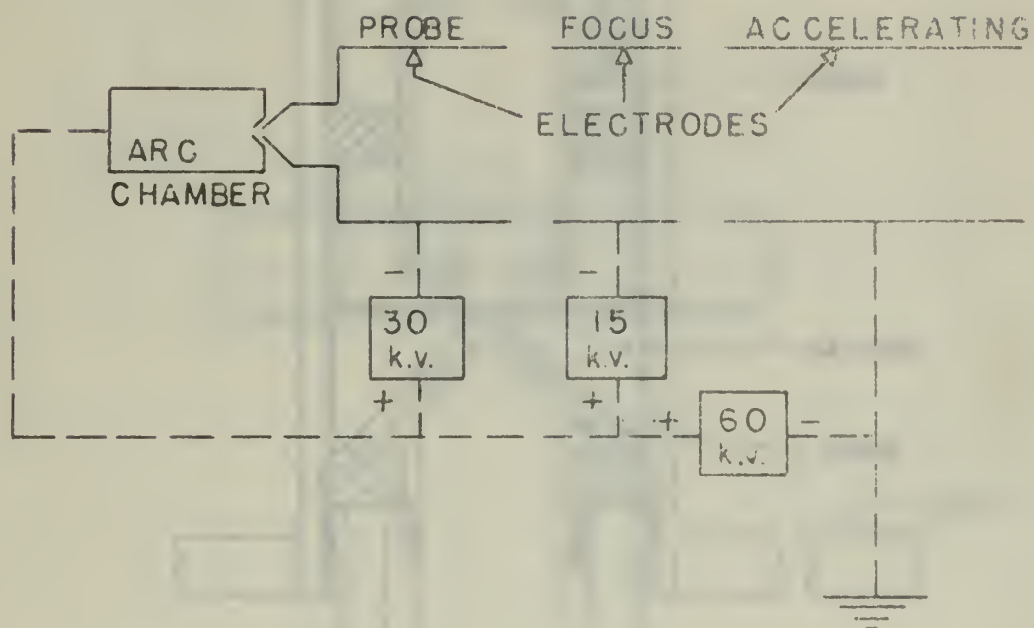
Reasons why the virtual-image source did not get more current through the system are obscure, just as the focusing characteristics of the injection system are, but indications are that the beam was too diffuse, certainly in size and probably also in energy, for it to be accelerated effectively on through the injection system. Smaller tubes

or other changes might improve performance somewhat, but it is quite likely the system prefers a real-image source to any virtual-image source that might be designed.

1. TROTT, J. B. and
TROTTER, J. B. (1967)
The Theory of Imaging Optics,
Vol. 1. The Invariant
Principle.
2. TROTT, J. B.
TROTTER, J. B. and
TROTTER, J. B. (1967)
The Theory of Imaging Optics,
Vol. 2. The Invariant
Principle.
3. TROTT, J. B.
TROTTER, J. B. and
TROTTER, J. B. (1967)
The Theory of Imaging Optics,
Vol. 3. The Invariant
Principle.
4. TROTT, J. B.
TROTTER, J. B. and
TROTTER, J. B. (1967)
The Theory of Imaging Optics,
Vol. 4. The Invariant
Principle.
5. TROTT, J. B.
TROTTER, J. B. and
TROTTER, J. B. (1967)
The Theory of Imaging Optics,
Vol. 5. The Invariant
Principle.
6. TROTT, J. B.
TROTTER, J. B. and
TROTTER, J. B. (1967)
The Theory of Imaging Optics,
Vol. 6. The Invariant
Principle.
7. TROTT, J. B.
TROTTER, J. B. and
TROTTER, J. B. (1967)
The Theory of Imaging Optics,
Vol. 7. The Invariant
Principle.
8. TROTT, J. B.
TROTTER, J. B. and
TROTTER, J. B. (1967)
The Theory of Imaging Optics,
Vol. 8. The Invariant
Principle.
9. TROTT, J. B.
TROTTER, J. B. and
TROTTER, J. B. (1967)
The Theory of Imaging Optics,
Vol. 9. The Invariant
Principle.
10. TROTT, J. B.
TROTTER, J. B. and
TROTTER, J. B. (1967)
The Theory of Imaging Optics,
Vol. 10. The Invariant
Principle.

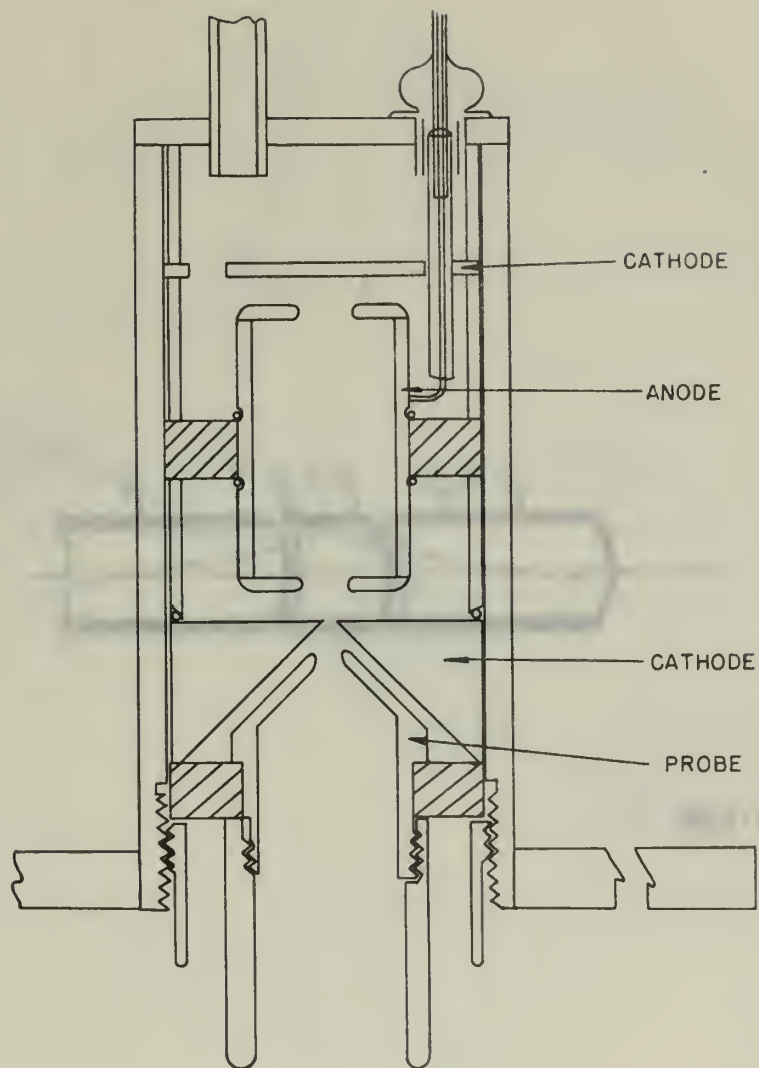
BIBLIOGRAPHY

1. Gow, J. D. and Foster, J. S., Jr. A HIGH-INTENSITY PULSED ION SOURCE,
The Review of Scientific Instruments,
Vol. 24, No. 8, pp 606-610,
August 1953
2. Penning, F. M. Physica 4, 71 (1937)
3. Hoyaux, M. and Dujardin, I. COMPARATIVE SURVEY OF ION GUNS,
Nucleonics Research Laboratories,
Ateliers de Constructions Electriques de Charleroi, Belgium
4. Pierce, J. R. THEORY AND DESIGN OF ELECTRON BEAMS,
D. Van Nostrand Company, 1949
5. Thonemann, P. C. Nature 158, 61 (1946)
6. Fowler, R. D. and Gibson, G. E. Phys. Rev. 46, 1075 (1934)
7. Field, L. M. Spangenberg, K. and Helm, R. CONTROL OF ELECTRON BEAM DISPERSION AT HIGH VACUUM BY IONS,
Elec. Comm. 24, No. 1, pp 108-121, March 1947
8. Zworykin, V. K. Morton, G. A. Ramberg, E. G. Hillier, J. and Vance, A. W. ELECTRON OPTICS AND THE ELECTRON MICROSCOPE,
John Wiley and Sons, Inc., 1948



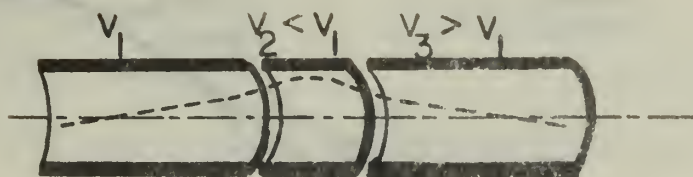
MU-9546

Fig. 1 Block Diagram of Ion Source.
 Diameter for Electrode Tubes, 2 in.;
 Lengths of Electrodes:
 probe, 2 in.;
 focus, 2.5 in.;
 accelerating, 4 in.



MU3409

Fig. 2 Cross Section of Arc Chamber



MU-9547

Fig. 3 Focusing Action of Three Electrodes



Figure 10.

Figure 10. A diagram showing a horizontal cylinder divided into three sections. The left section is labeled $u = v$, the middle section is labeled $v = w$, and the right section is labeled w . A horizontal line runs through the center of the cylinder.

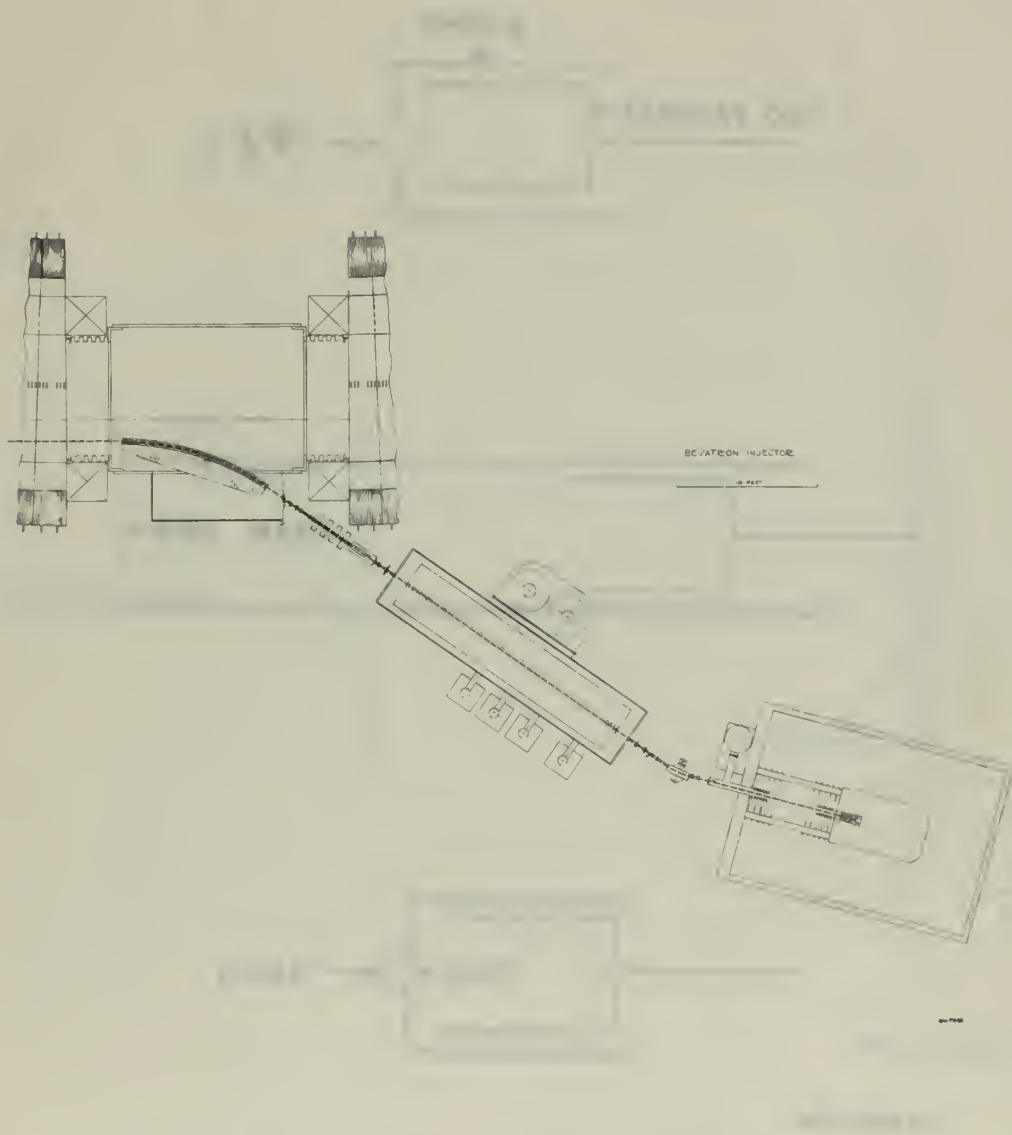
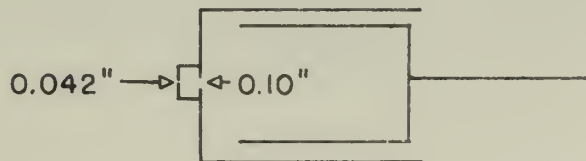
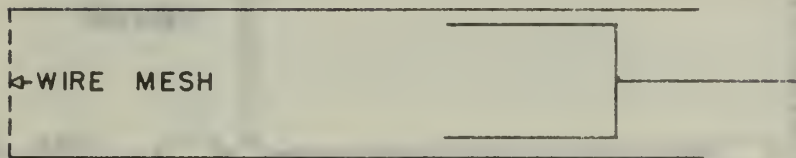
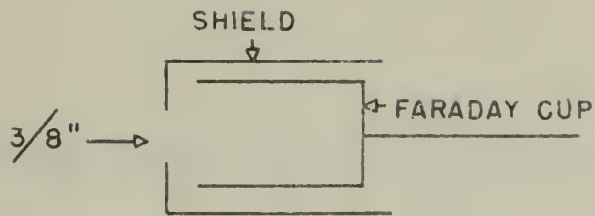


Fig. 4 Block Diagram of Bevatron Injection System

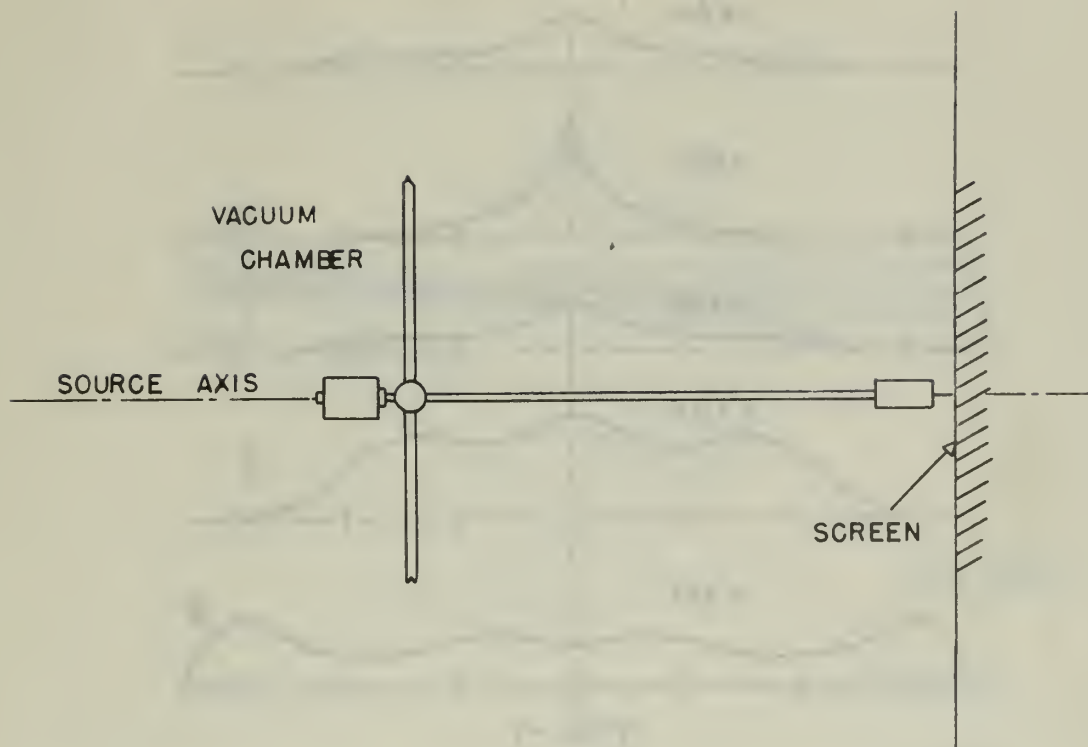


MU-9548

Fig. 5 Original Faraday Cup, Shield with $3/8$ -inch Hole

Fig. 6 Faraday Cup, Long Shield

Fig. 7 Faraday Cup, Special Shield

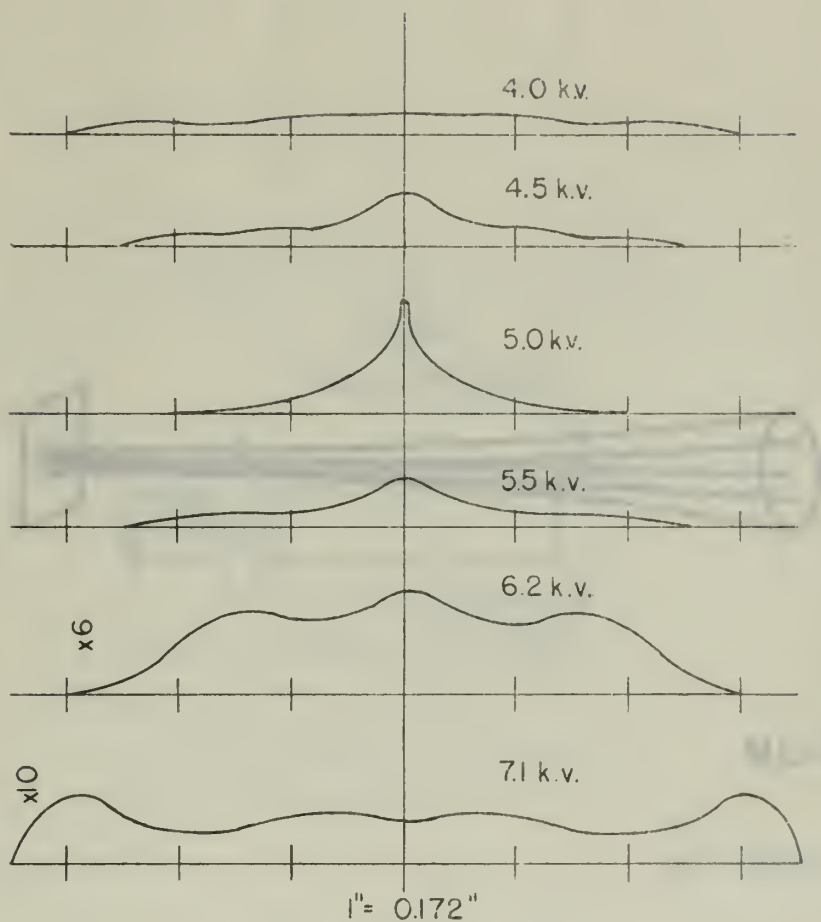


MU-9549

Fig. 8 Mechanical Advantage of Cup Movement

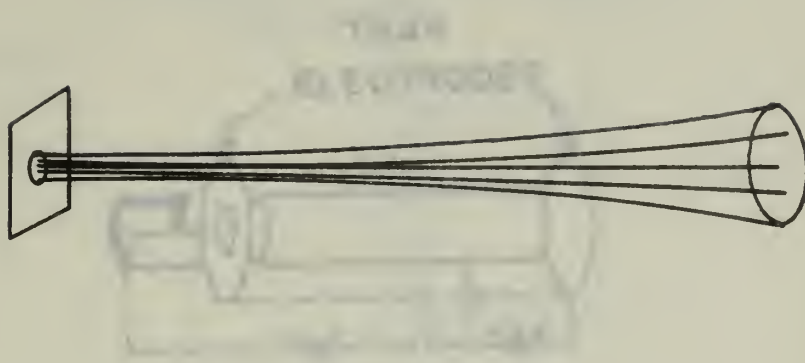


Figure 1. Schematic diagram of the mechanical system.



MU-9550

Fig. 9 Beam-Intensity Cross Sections,
Variable-Focus Electrode Voltage



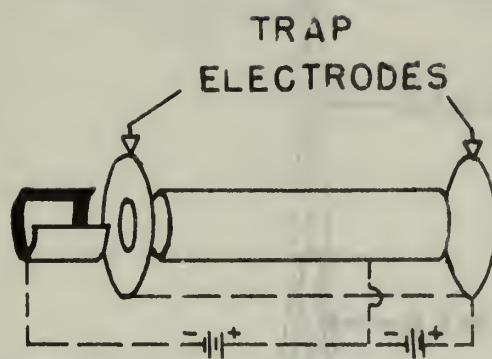
MU-9551

Fig. 10 Spreading of Originally Parallel Proton Beam Due to Space Charge



100-UM

FIG. 1. Schematic diagram of the device for measuring the length of the rod.



MU-9552

Fig. 11 Ion Trap



507-114

507-114

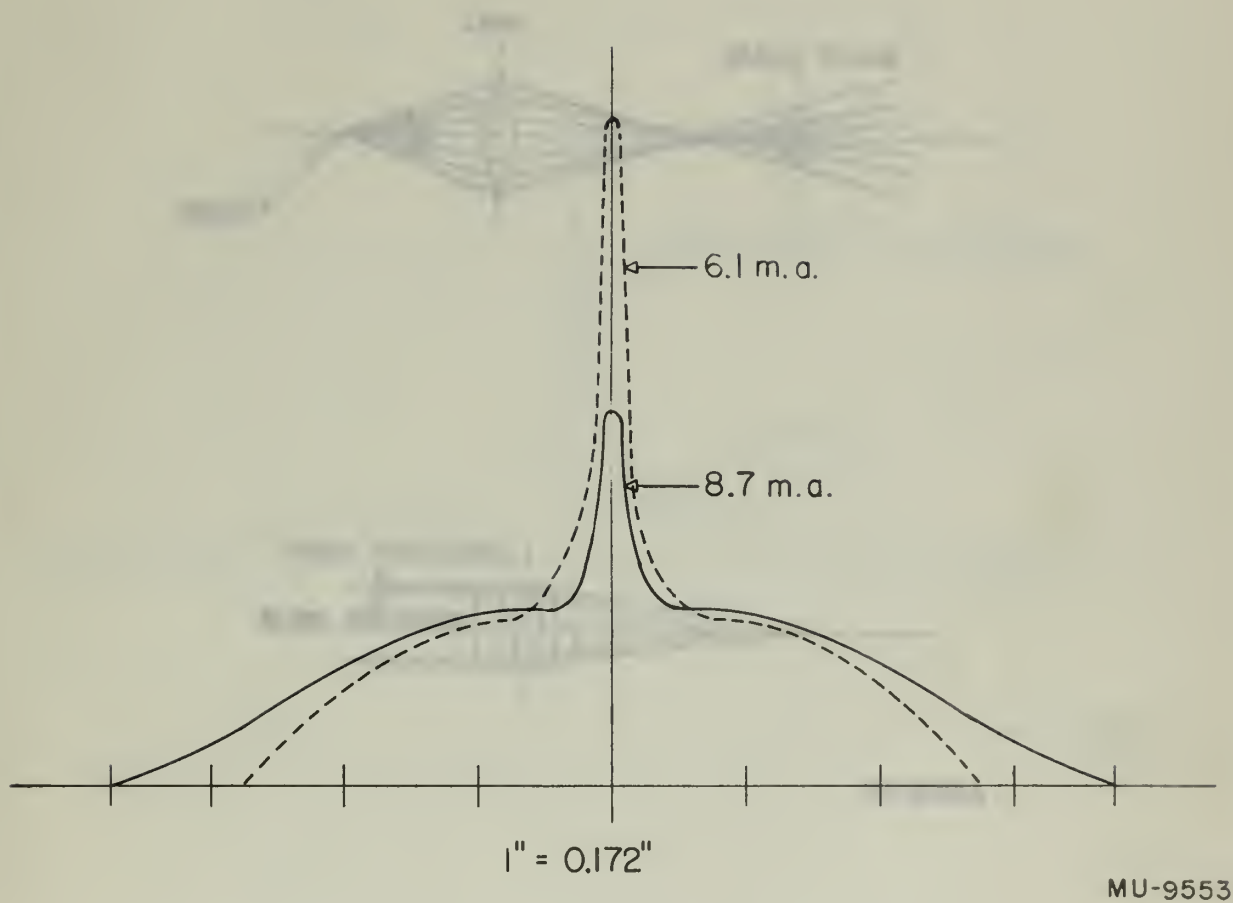
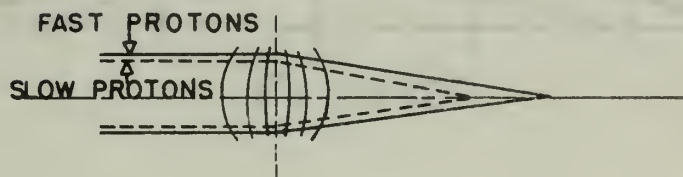
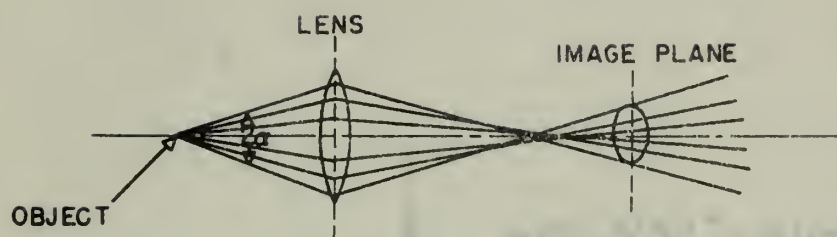


Fig. 12 Beam-Intensity Cross Sections,
Space-Charge Effects



MU-9554

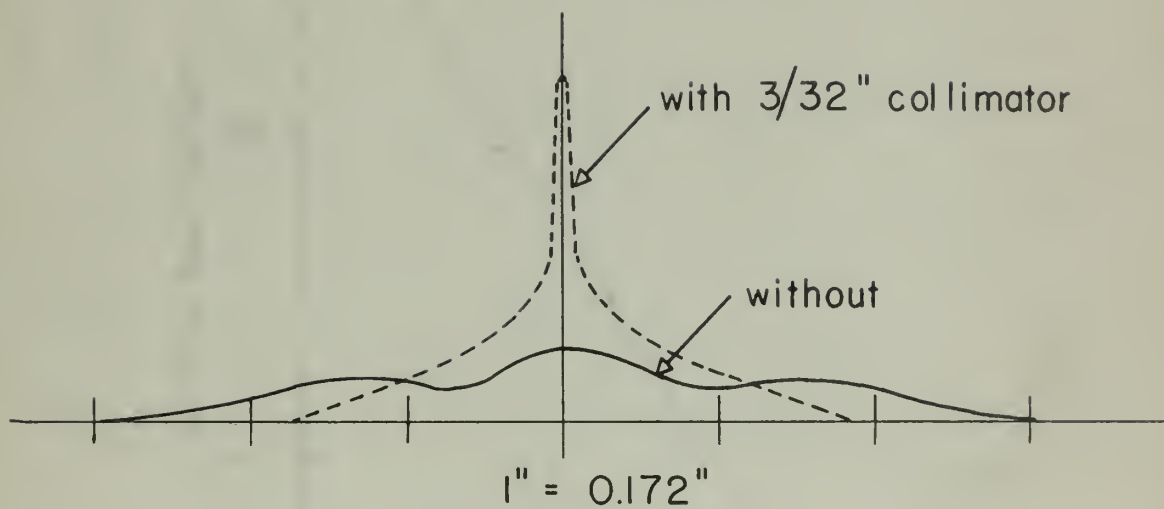
Fig. 13 Spherical Aberration

Fig. 14 Chromatic Aberration



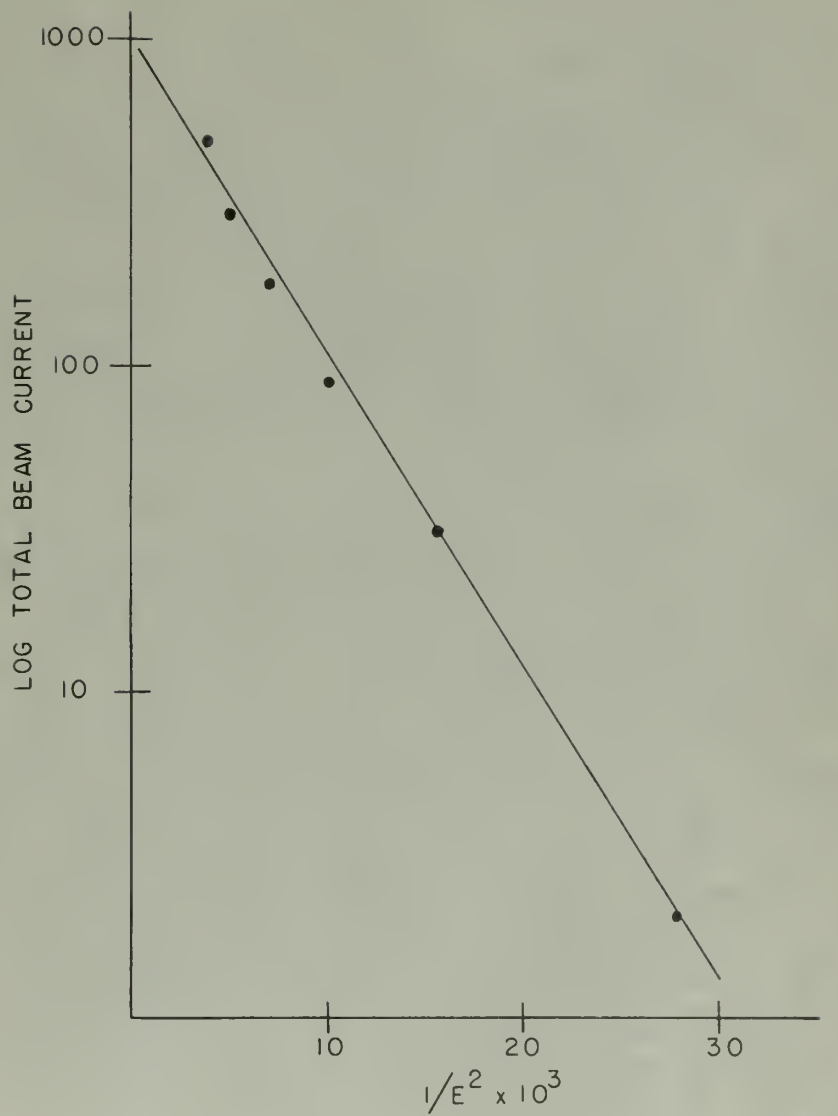
FIGURE 1

FIGURE 1
FIGURE 2



MU-9555

Fig. 15 Beam-Intensity Cross Sections,
Aberration Effects



MU-9556

Fig. 16 Total Current Versus Energy, Coulomb Losses
(E is energy of Accelerating Electrode)

JL 19 56

INTERLIB

Naval Research Lab

28473

Thesis
S765

Stone

Experiments on
improving the efficiency
of the bevatron ion
source.

JL 19 56

INTERLIB

28473

Thesis
S765

Stone

Experiments on improving the
efficiency of the bevatron
ion source.

thesS765

Experiments on improving the efficiency



3 2768 002 02042 2

DUDLEY KNOX LIBRARY